THE JOURNAL OF PROSTHETIC DENTISTRY

RESEARCH AND EDUCATION

Complete arch implant scans with standard scan bodies versus scannable healing abutments on scanning accuracy, scanning time, and number of photograms: A comparative clinical study

Miguel Gómez-Polo, DDS, PhD,[a] Rocío Cascos, DDS, PhD,[b] Rocío Ortega, DDS, PhD,[c] Abdul B. Barmak, MD,[d] and Marta Revilla-León, DDS, MSD, PhD[e]

ABSTRACT

Statement of problem. Digital scans for complete arch implant fixed dental prostheses are typically performed using implant scan bodies (ISBs). Scannable healing abutments may be an alternative to ISBs. However, evidence on the accuracy, scanning time, and number of photograms of digital scans using scannable healing abutments remains uncertain.

Purpose. The purpose of this clinical study was to evaluate the scanning accuracy, scanning time, and number of photograms of scannable healing abutments of several heights in comparison with standard ISBs.

Material and methods. A reference stone cast was obtained from a patient with 7 maxillary implants from a splinted open-tray conventional impression. It was digitized by using a laboratory scanner (E4 Scanner). A milled titanium bar was manufactured, and passive fit was evaluated clinically and radiographically. Three groups (n=15) were determined based on the devices used during the intraoral scanning procedure (TRIOS 4): standard ISB (Scanbody 2800) (Group STD), 5-mm height scannable healing abutment (TissueShaper 5 mm) (Group TS5), and 7-mm height scannable healing abutment (TissueShaper 7 mm) (Group TS7). The implant abutment discrepancy between the platform of the abutments of the digitized reference cast and the intraoral scans from the different groups were calculated. Maximum deviation (highest value of misfit per scan) and overall deviations (mean of all the deviations of the scan) were considered. The scanning time and number of photograms were registered. The 1-way ANOVA and Tukey tests were used to analyze trueness. The Levene test was used to analyze the precision. ANOVA and the post hoc Tukey test were used to evaluate the scanning time and numbers of photograms (α=.05).

Results. Significant trueness differences were found in the overall and maximum misfit among the groups (P<.05). Significant precision discrepancies were revealed in the maximum misfit (P<.05) but not in the overall misfit (P=.56). The highest deviations were in the STD group (overall: 94 ±6 μm; maximum misfit: 172 ±24 μm), followed by TS5 (overall: 72 ±10 μm; maximum misfit: 112 ±15 μm) and TS7 (overall: 63 ±9 μm; maximum misfit: 91 ±20 μm). Significant differences in scanning time and number of photograms were found between the STD group and both the TS5 and TS7 groups (P<.01). The longest scanning time (129.9 ±16.7 s) and highest number of photograms (1322 ±150 photograms) were in the STD group in comparison with TS5 (71.7 ±10.8 s; 805 ±104 photograms) and TS7 (77.3 ±0.9 s; 764 ±119 photograms).

Conclusions. The tested scannable healing abutments improved the accuracy and decreased the scanning time and number of photograms in complete arch implant digital scans recorded by using the IOS assessed. (J Prosthet Dent xxxx;xxx:xxx-xxx)

This research did not receive any specific grant from funding agencies in the public, commercial, or not-for-profit sectors.
The authors did not have any conflict of interest, financial or personal, in any of the materials described in this study.

[a]Associate Professor, Department of Conservative Dentistry and Prosthodontics, School of Dentistry, Complutense University of Madrid (UCM), Madrid, Spain; and Director, Postgraduate Program of Advanced in Implant-Prosthodontics, School of Dentistry, Complutense University of Madrid (UCM), Madrid, Spain.
[b]Assistant Professor of Postgraduate Program of Advanced in Implant-Prosthodontics, School of Dentistry, Complutense University of Madrid (UCM), Madrid, Spain; and Adjunct Professor Department of Prosthetic Dentistry, School of Dentistry, European University of Madrid, Madrid, Spain.
[c]Assistant Professor, Postgraduate Program of Advanced in Implant-Prosthodontics, School of Dentistry, Complutense University of Madrid (UCM), Madrid, Spain; and Associate Professor Department of Prosthetic Dentistry, School of Dentistry, European University of Madrid, Madrid, Spain.
[d]Assistant Professor, Clinical Research and Biostatistics, Eastman Institute of Oral Health, University of Rochester Medical Center, Rochester, NY.
[e]Affiliate Professor, Graduate Prosthodontics, Department of Restorative Dentistry, School of Dentistry, University of Washington, Seattle, Wash.; Faculty and Director, Research and Digital Dentistry, Kois Center, Seattle, Wash; and Affiliate Professor, Graduate Prosthodontics, Department of Prosthodontics, School of Dental Medicine, Tufts University, Boston, Mass.

Clinical Implications

The scannable healing abutments tested may be used to record implant positions in complete arch implant scans by using the IOS evaluated, improving the scanning accuracy and reducing the scanning time and number of photograms.

Digital workflows have been introduced in dentistry,[1,2] with intraoral scanners (IOSs) used to register not only teeth and soft tissues but also dental implants.[3–5] Factors identified as influencing factors on the accuracy of implant digital scans[6–8] include operator-related factors,[8–11] ambient lighting conditions,[12–14] scanning pattern,[15–18] and ISB design,[19–21] Numerous recent studies[22–33] have aimed to quantify the accuracy of complete arch implant digital scans, as complete arch implant digital scans have been considered insufficiently accurate to obtain reliable digital casts.[34]

Accurately reproducing the implant position is essential for successful implant-supported prostheses,[34,35] especially in long-span or complete arch implant-supported dental prostheses (CIDPs).[33,36] A passive fit has been associated with a lack of mechanical or biological complications.[37,38] As a consequence, several methodologies have been described to improve the accuracy of complete arch implant digital scans.[39,40]

In digital workflows using IOSs, the 3D position of the implants is transferred by means of implant scan bodies (ISBs).[19–21] Previous studies have aimed at determining the influence of the ISB characteristics on the accuracy of implant scans recorded by using IOSs.[41–43] Although some parameters related to the ISBs have been identified as influencing factors,[6,41–44] the evidence is still scarce; as a result, these studies have concluded that further research with this scope is needed.

In addition to standard designs, alternative ISB configurations have been proposed, such as horizontal ISBs[22,45] or those intended for use with healing abutments.[46] Recently, scannable healing abutments have been introduced. While using healing abutments to replicate implant position is not a new technique, the accuracy of this method remains uncertain.[47–49] Moreover, much of the existing research on ISBs is based on in vitro studies, highlighting the need for clinical trials to better assess performance. Additionally, previous studies using similar methodologies have incorporated scanning time and the number of photograms into their data collection.[16,18,50–52] While these factors are less critical than accuracy for the prosthesis, longer scanning time may reduce patient comfort, and a higher number of images may result in larger file sizes. The present clinical study aimed to analyze the accuracy (trueness and precision), scanning time, and number of photograms of complete arch intraoral implant scans obtained with standard ISBs or scannable healing abutments (5- or 7-mm height). The null hypotheses were that no differences would be found in the scanning trueness and precision, scanning time, and number of photograms of complete arch intraoral implant scans obtained with standard ISBs or scannable healing abutments.

MATERIAL AND METHODS

The inclusion criteria involved patients with a completely edentulous arch with 6 to 8 osseointegrated implants complying with success criteria, older than 18 years old, and in good medical conditions (American Society for Anesthesiologists type I or II). The exclusion criteria included patients with limited mouth opening or with peri-implantitis. The research protocol had been approved by an International Review Board Committee (22/645-E).

A patient with an edentulous maxillary arch was selected for the study. The patient had 7 healthy dental implants placed in the maxillary arch in the right first molar, right and left first premolar, right and left lateral incisor, left canine, and left second molar positions. The maxillary arch presented an interim screw-retained complete arch implant-supported prosthesis screwed onto transepithelial multiunit abutments. The patient was informed of the study's methodology, questions were resolved, and an informed consent was signed.

For the reference cast, a conventional impression was made by following a modified shim open tray splinted technique.[53] The open-tray implant impression abutments (Impression Coping Open Tray Transepithelial 4.8 Non-Eng; Avinent Implant System) were hand tightened to the implant abutments. A preliminary open-tray impression was obtained by using a perforated prefabricated plastic tray. An implant analog was positioned to each implant impression abutment, and the impression was poured with a gingival mask (Gi-Mask; Coltène) and Type IV dental stone (Fujirock EP; GC) according to the manufacturer recommendations. The preliminary cast was retrieved after the dental stone had completely set.

The preliminary stone cast was digitized to design a splinting framework for the definitive implant impression. First, ISBs (transepithelial scan body 2800; Avinent Implant System) were hand tightened on the implant abutment analogs as endorsed by the manufacturer. Then, a calibrated desktop scanner (E4 Desktop Scanner; 3Shape A/S) was used to digitize the cast. Afterwards, a splinting framework was designed (DentalCAD 3.1; exocad GmbH). The design included 7 cylinders, 1 per implant, connected by a bar. This framework was milled (CAD/CAD Idodentine disc;

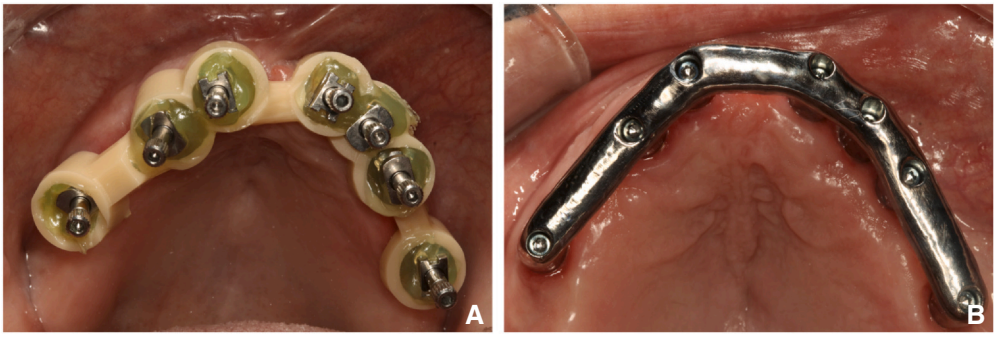

Figure 1. A, Milled framework and splinted open-tray copings for double-splinted conventional impression. B, Titanium milled bar for passive fit evaluation.

Unidesa) and saved for the definitive implant impression. An open-tray photopolymerized acrylic resin custom tray was also manufactured (Kiero Planchas Tray; Kuss Dental).

The definitive conventional implant impression was obtained. An open-tray implant impression abutment was screwed on each implant abutment. The milled framework was splinted to the implant impression abutments by using photopolymerizing material (Conlight; Kuss Dental) (Fig. 1A). After the complete polymerization of the splinting material, the conventional implant impression was completed by using the open-tray custom tray and a polyether impression material (Impregum; 3M ESPE). The impression was retrieved after the recommended working time and poured with Type IV dental stone (Fujirock EP; GC) to obtain the definitive implant stone cast.

The definitive implant stone cast was digitized by using the same calibrated desktop scanner. On each implant abutment analog, a new ISB (transepithelial scan body 2800; Avinent Implant System) was tightened at 10 Ncm according to the manufacturer's recommendations. The cast was digitized, and the STL file was imported into a software program (DentalCAD 3.1; exocad GmbH). A CAD object of the ISB was aligned with each ISB of the digitized definitive cast. Then, the definitive virtual implant cast was obtained.

A screw-retained implant-supported framework was designed and manufactured from the definitive implant cast to check the accuracy of the definitive implant cast. The framework was manufactured in Ti grade V (Colado CAD Ti5 Disc; Ivoclar AG) using a milling machine (PrograMill PM7; Ivoclar AG) (Fig. 1B). The fit of the implant-supported Ti framework was first checked in the definitive implant stone cast using the alternative pressure test, the Sheffield test, and visual and tactile (with an explorer) verification. The same procedure was performed in the patient's mouth, where periapical radiographs were also obtained with the parallelization method.[18] After checking for adequate implant framework fit, the definitive virtual implant was considered as the reference cast; therefore, linear and angular deviations of the specimens were assessed through comparison with this cast. Three groups were established based on the type of ISB used: standard ISBs (STD group) and scannable healing abutments with heights of 5 mm (TS5 group) and 7 mm (TS7 group). Complete arch digital scans for all the groups were acquired intraorally using a calibrated intraoral scanner (TRIOS4, v.22.2; 3Shape A/S). Calibration of the IOS was performed according to the manufacturer's instructions at the start of each group. All scans were conducted by a single operator (M. G-P) with 8 years of experience using IOS systems and under controlled temperature and lighting conditions (1000 ±50 lux).[12–14] The number of photograms and the scanning time (seconds) for each specimen were reported by the IOS software program.

Seven new ISBs were tightened to 10 Ncm to the implant abutments, as endorsed by the manufacturer. They were not adjusted or disturbed until the data acquisition process was completed. The zig-zag scanning protocol was followed.[15–17,54] All the scans started at the implant abutment located in the first right molar position. The IOS head was advanced from buccal to lingual, recording the IBSs' surfaces and soft tissues until the scan was completed. All the scans were evaluated, and those that included mistakes or areas that were not properly recorded were excluded and repeated.

For the scannable healing abutments groups (TS5 and TS7 groups), metal hemispherical dome-shaped ISBs were used (Tissue Shaper; MedicalFit). Their design includes 2 oval flat bevels corresponding to the hemisphere segmentation at 35 degrees from the x-axis. (Fig. 2) This angulation allowed the IOSs to capture the flat bevels from an occlusal view during the scan and facilitated the fitting of the virtual replicas during the software procedure. Additional indentations were included to identify whether the ISB was of 5 mm (one additional circle plane) or 7 mm (two additional circle plane) height. In the TS5 group, a 5-mm height scannable healing abutment (Tissue shaper 5 mm; MedicalFit) was used. In the TS7 group, a 7-mm height

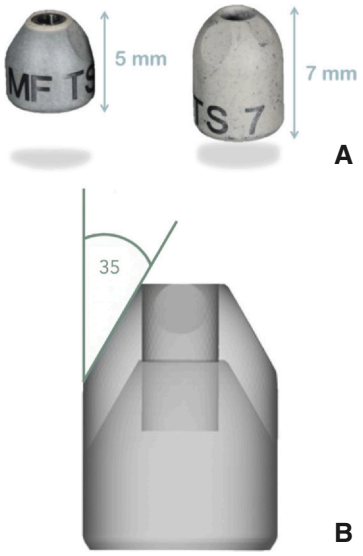

Figure 2. A, Scannable healing abutments of 5 mm and 7 mm height. B, Axial view of scannable healing abutment design.

scannable healing abutment (Tissue shaper 7 mm; MedicalFit) was used (Fig. 3A-D). For the STD group, a 10-mm height cylindrical metal-polyetheretherketone (PEEK) ISBs was used (Scan body 2800; Avinent Implant System). A geometrical bevel that was oriented to the lingual to maximize the scanning accuracy was included in this design (Fig. 3E, F). Fifteen scans per group were performed. The sample size was estimated considering previous studies.[11–18,21,28–33]

The deviations at the implant abutment level were calculated. First, the circumferences corresponding to the CAD bar's connections at the implant abutment were selected using the software program tools (Meshmixer v3.5; Autodesk) (Fig. 4). The STL file with the 7 circumferences was named "reference connections file" (RCF). The same procedure was followed to obtain the circumferences of the control and test groups. In TS5 specimens, a CAD object of the corresponding ISB was superimposed (Fig. 5A, B). Then, the circumferences of the TS5 ISBs at the abutment level were selected by using the software program tools. An STL file was saved and codified with the group's name and number. The file with the circumferences of the TS5 ISBs and the RCF were then aligned by best fit (Fig. 5C). Once superimposed, the software program tools were used to obtain the highest deviation value between the connections of all the implants (Fig. 6A). This was considered as the maximum misfit of the specimen. Then, this procedure was repeated for each implant individually, obtaining the maximum discrepancy per implant (Fig. 6B). These values were used to obtain the overall misfit, calculating the average of the discrepancies of all 7 of the implants on each scan. This procedure was repeated for all the specimens of the control, TS5, and TS7 groups.

A software program (IBM SPSS Statistics, v26; IBM Corp) was used for the statistical analysis of the study data (α=.05). The Shapiro-Wilk test was performed to evaluate the normal distribution of the data for each studied variable (overall deviation (P=.290), maximum deviation P=.244), scanning time (P=.002), and number of photograms (P=.274). One-way ANOVA followed by the Tukey pairwise comparisons test was used to assess

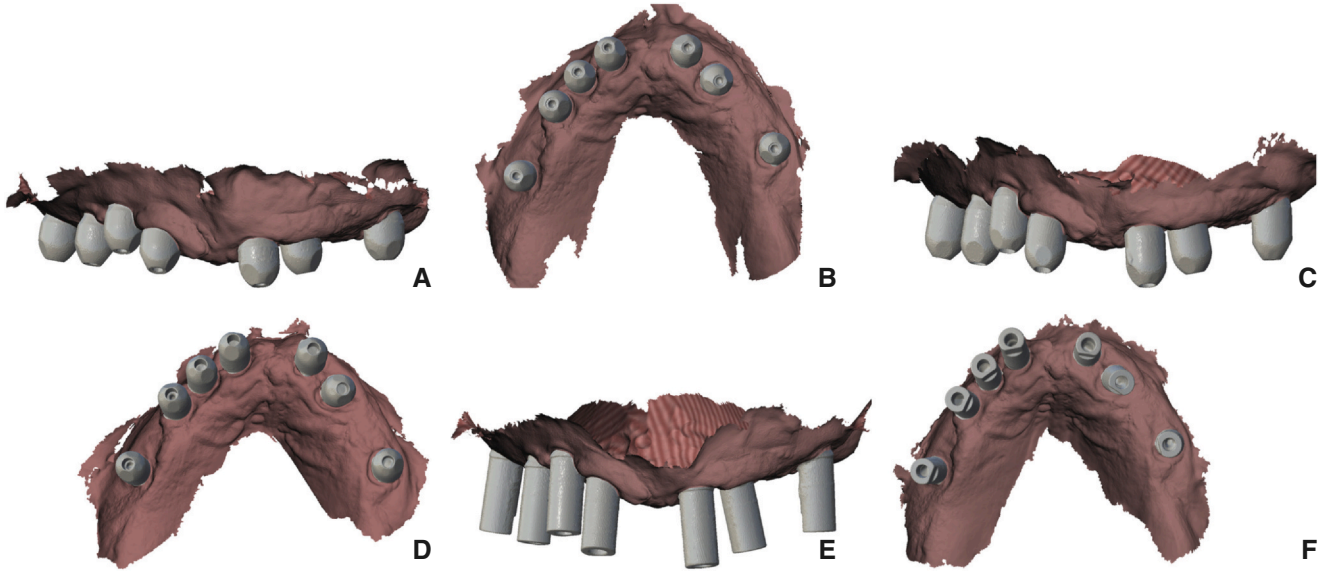

Figure 3. A, B, Representative example of TS5 group scans (frontal and occlusal view). C,D, Representative example of TS7 group scans (frontal and occlusal view). E,F, Representative example of STD group scans (frontal and occlusal view). STD, standard implant scan body (Scanbody 2800); TS5, 5-mm height scannable healing abutment (TissueShaper 5 mm); TS7, 7-mm height scannable healing abutment (TissueShaper 7 mm).

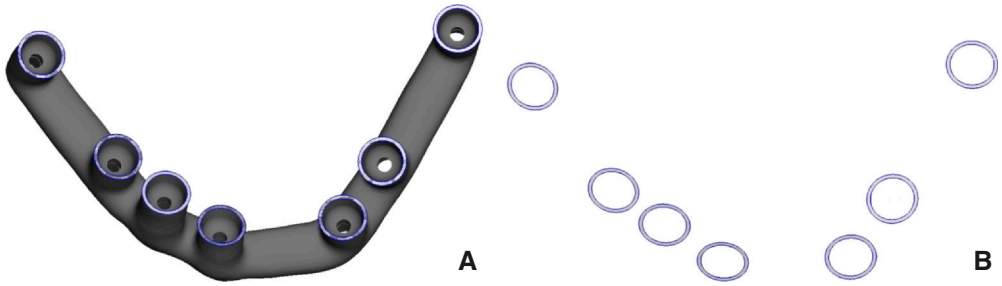

Figure 4. A, Representative figure of selection of bar connections. B, Bar connections once bar deleted.

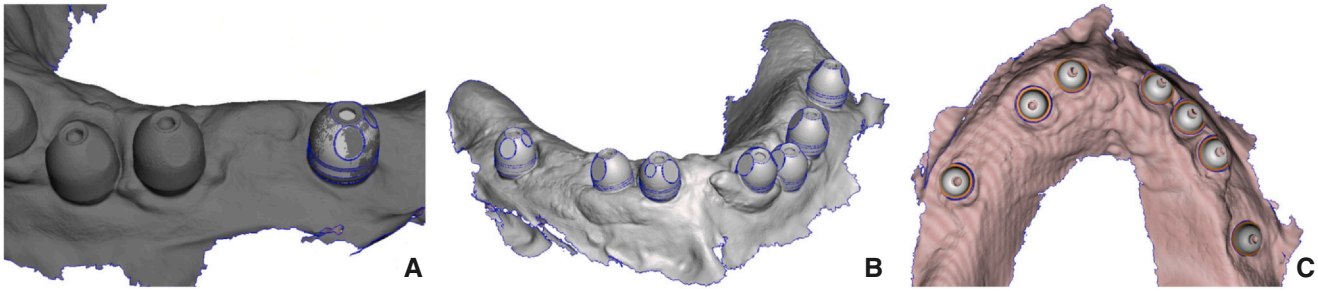

Figure 5. A, Representative figure of TS5 CAD object superimposition. B, Representative figure of model with TS5 CAD objects superimposed. C, Representative model with TS5 connections selected. CAD, computer-aided design; STD, standard implant scan body (Scanbody 2800); TS5, 5-mm height scannable healing abutment (TissueShaper 5 mm); TS7, 7-mm height scannable healing abutment (TissueShaper 7 mm).

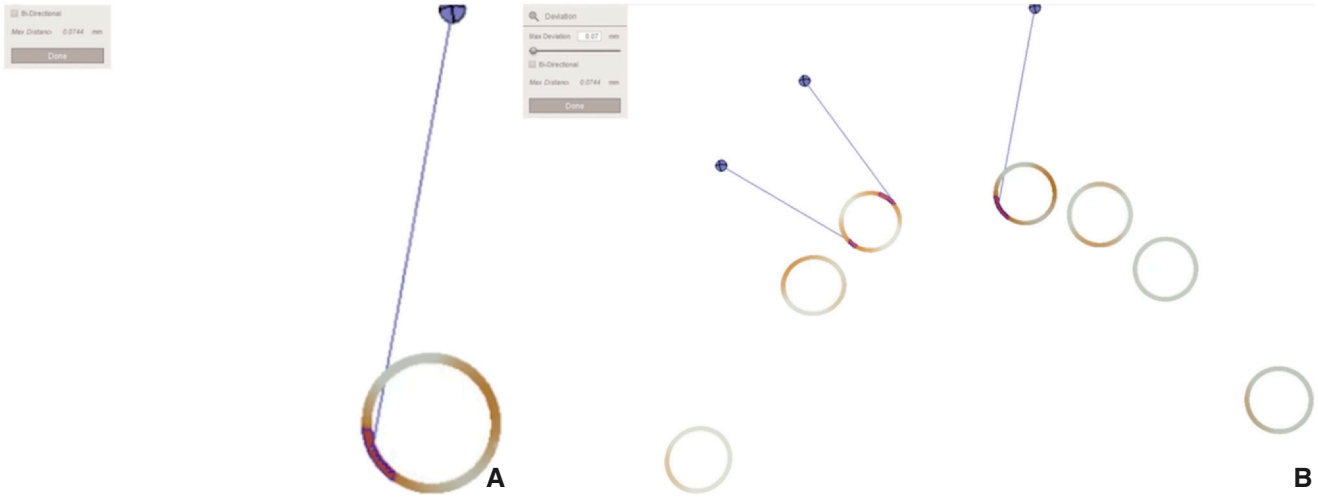

Figure 6. A, Representative figure of highest deviation of one specimen (123 µm) in implant located in left canine position. B, Representative figure of individual highest deviation per implant (74 µm).

trueness, scanning time and number of photograms. The Levene test was used for precision analysis.

RESULTS

For the overall deviations, 1-way ANOVA (F=48.28, df1=2, df2= 27.1, *P*<.01) demonstrated significant trueness differences among the groups tested. The Tukey post hoc test showed significant trueness differences between the STD group and both the TS5 and TS7 groups (*P*<.01). Significant trueness differences were also found between the TS5 and TS7 groups (*P*=.018). For precision, the Levene test did not show significant differences among the groups tested (*P*=.562). The mean ±SD of the overall deviations was 94 ±6 µm for the STD group, 72 ±10 µm for the TS5 group, and 63 ±9 µm for the TS7 group (Table 1, Fig. 7).

Regarding the maximum deviation analysis, 1-way ANOVA (F=48.28, df1=2, df2=27.1, *P*<.001) revealed significant maximum deviation among the groups tested. Additionally, the Tukey post hoc test showed statistical differences among all the groups tested

Table 1. Descriptive data of deviations, scanning time, and number of photograms reported in groups tested

Group	Overall Deviations (Mean ±SD) (Trueness ±Precision) (μm)	Maximum Deviation Per Scan (Mean ±SD) (Trueness ±Precision) (μm)	Scanning Time (Seconds)	Number of Photograms
STD	94 ±6	172 ±24	129.9 ±16.7	1322 ±150
TS5	72 ±10	112 ±15	71.7 ±10.8	804 ±105
TS7	63 ±9	91 ±20	77.3 ±10.9	764 ±119

SD, standard deviation; STD, standard implant scan body (Scanbody 2800); TS5, 5-mm height scannable healing abutment (TissueShaper 5 mm); TS7, 7-mm height scannable healing abutment (TissueShaper 7 mm).

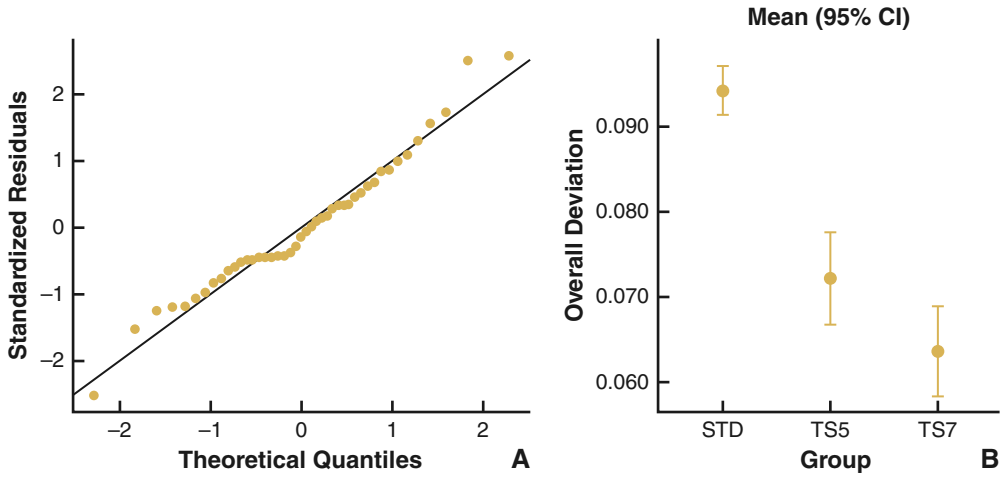

Figure 7. A, Q-Q graphic of sample distribution (overall deviations). B, Plot of overall deviations results (mean 95% CI). CI, confidence interval; STD, standard implant scan body (Scanbody 2800); TS5, 5-mm height scannable healing abutment (TissueShaper 5 mm); TS7, 7-mm height scannable healing abutment (TissueShaper 7 mm).

(*P*<.05). The Levene test reported significant precision differences among the groups (*P*=.045), with STD being more precise than the TS5 and TS7 groups. The mean ±SD of the maximum deviation was 172 ±24 mm for the STD group, 112 ±15 mm for the TS5 group, and 91 ±20 mm for the TS7 group (Table 1, Fig. 8).

Regarding the scanning time analysis, the 1-way ANOVA found significant differences (F 67.6, df1 2, df2 27.2, *P*<.001) among the groups tested. The Tukey post hoc test showed that differences were found between the STD group (129.9 ±16.7 s) and both TS5 (71.7 ±10.8 s) and TS7 groups (77.3 ±10.9 s) (*P*<.001). No

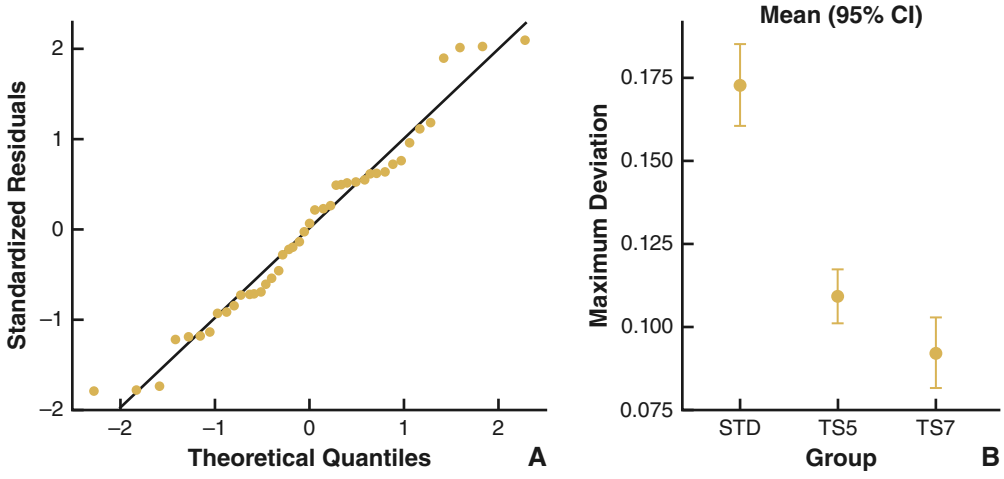

Figure 8. A, Q-Q graphic of sample distribution (maximum deviations). B, Plot of maximum deviations results (mean 95% CI). CI, confidence interval; STD, standard implant scan body (Scanbody 2800); TS5, 5-mm height scannable healing abutment (TissueShaper 5 mm); TS7, 7-mm height scannable healing abutment (TissueShaper 7 mm).

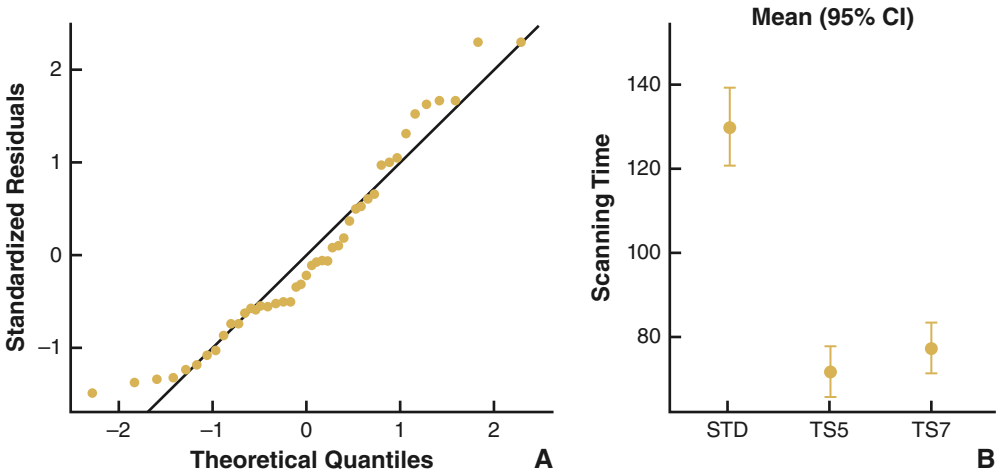

Figure 9. A, Q-Q graphic of sample distribution (scanning time). B, Plot of scanning time results (mean 95% CI). CI, confidence interval; STD, standard implant scan body (Scanbody 2800); TS5, 5-mm height scannable healing abutment (TissueShaper 5 mm); TS7, 7-mm height scannable healing abutment (TissueShaper 7 mm).

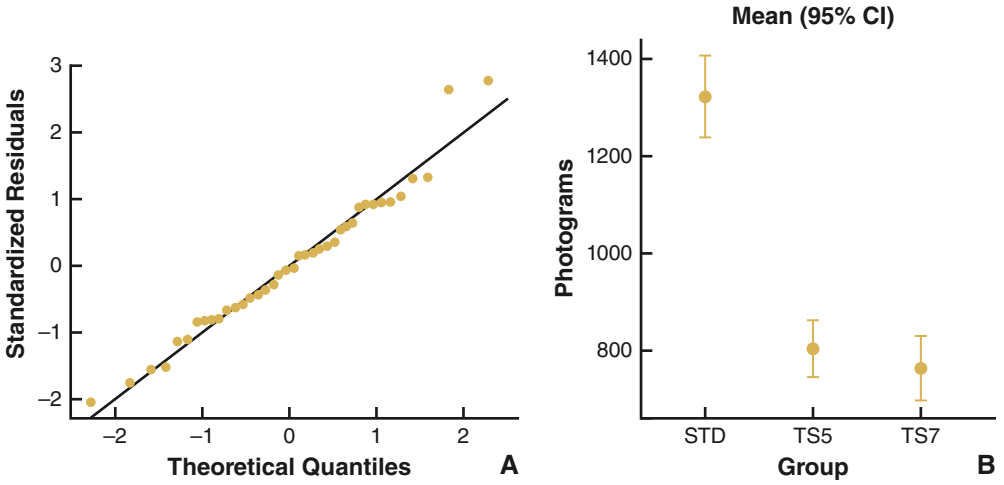

Figure 10. A, Q-Q graphic of sample's distribution (number of photograms). B, Plot of number of photograms results (mean 95% CI). CI, confidence interval; STD, standard implant scan body (Scanbody 2800); TS5, 5-mm height scannable healing abutment (TissueShaper 5 mm); TS7, 7-mm height scannable healing abutment (TissueShaper 7 mm).

significant differences were found between the TS5 and TS7 groups (P=.47) (Table 1, Fig. 9).

For the number of photograms, the Tukey post hoc test found statistically significant differences among the STD groups (1322 ±150 photograms) and both the TS5 (804 ±105 photograms) and TS7 groups (764 ± 119 photograms) (P<.001). No statistically significant differences were found between the TS5 and TS7 groups (P=.66) (Table 1, Fig. 10).

DISCUSSION

Based on the results obtained in the present investigation, the null hypotheses that no differences would be found in scanning trueness and precision, scanning time, and number of photograms of complete arch intraoral implant scans obtained with standard ISBs or scannable healing abutments were rejected. The use of scannable healing abutments influenced the accuracy, scanning time, and number of photograms of complete arch implant digital scans recorded by using the IOS tested.

Previous studies have assessed the scanning accuracy of complete arch implant scans recorded by using IOSs. However, 2 factors of the present study differ from most of these previous studies evaluating the same parameters in similar situations: the clinical conditions and the measurement method used to assess the scanning discrepancies. Most of the previous studies were performed under in vitro conditions, where the reference file and cast were obtained by measuring the definitive

cast with desktop scanners,[27,48] industrial scanners,[28] or coordinate measuring machines.[25] These methods cannot be included in clinical studies, as the devices cannot be used intraorally. The only comparable approach has been tested on cadaveric models.[8,49] For this clinical study, the digital reference cast was obtained from the digitization of the definitive implant cast acquired from a double-splinted conventional implant impression. As this was an essential point in the study methodology, a verification milled titanium framework was manufactured, and its passive fit was clinically evaluated by visual, radiographic, and tactile tests.

To the best of the authors' knowledge, the methodology used to evaluate the discrepancies has not been used in previous research, which typically used the Euclidean distances and angulations[53,54] or 3D comparison of ISBs surfaces to calculate the root mean square (RMS) error.[26,27] A recent study also proposed the inclusion of the virtual Sheffield test.[52] The chosen assessment method was intended to quantify the maximal linear discrepancy between the platforms of the abutments in the digital scans and the framework where the passive fit takes place so that it may be more easily interpreted. Nevertheless, further studies specifically focused on evaluating and correlating the different measuring methods are needed.

Two parameters were measured in the present study: the maximum discrepancy (the highest value of misfit per scan) and the overall discrepancies (the mean of all the deviations of the scan). Theoretically, the overall discrepancy would provide a more general value of the accuracy of the scan. However, the maximum discrepancy may be more representative of the clinical situation. Nonetheless, the results obtained from both parameters are valuable and provide complementary information. Previous studies have reported the trueness and precision of the complete arch implant scans recorded by using IOSs. Several parameters have been selected for measuring scanning accuracy, such as 3D RMS error discrepancies. These parameters can be used to compare groups, but the clinical interpretations of the reported discrepancies are challenging. A systematic review reporting RMS error discrepancies obtained trueness data ranging from 35 to 581 μm and precision data varying from 5 μm to 355 μm.[34]

As an alternative to the RMS measurement method, linear and angular deviations among implants have been used to assess scanning accuracy.[25–28,55–58] This technique may provide more quantifiable values. Nevertheless, although some thresholds have been proposed (up to 200-μm in linear and up to 0.4 degrees in angular deviations),[59,60] the clinical implications of such linear and angular discrepancies remain unknown. Some recent in vitro studies have reported linear deviations ranging from −12 ±26 μm to 230 ±85 μm and angular discrepancies varying from 0.25 ±0.24 to 1.69 ±0.59 degrees.[25–28,61,62] Similarly, in vivo studies have reported linear deviations ranging from −20 ±63 μm to −19 ±87 μm and angular deviations varying from 0.4 ±0.05 to 0.84 ±0.29 degrees.[15,29,30] Nevertheless, these data must be carefully compared with those obtained in the present study, given the differences in the research methodology.

Statistically significant differences in trueness and precision were found. In trueness, they were reported in both parameters, overall and maximum discrepancy, between both the STD and both the TS5 and TS7 groups; in precision, they were only found in the maximum discrepancy. The magnitude of the differences was higher in the maximum discrepancy. This was logical since the average of the values is found in the overall calculation, so the best values per sample will compensate for the higher discrepancies. Considering the obtained results, using scannable healing abutments like the one used in the present study may significantly improve the accuracy in complete arch implant digital scans.

The scanning time and number of photograms have also been evaluated in previous studies of digital scans with IOSs. Both variables used to have a positive correlation, and a higher number of photograms implies a higher time. In the present results, the STD group showed a statistically significant longer scanning time and greater number of photograms. Scanning with shorter ISBs implied less manipulation of the scanning head, as all the information of the ISB can almost be reported in a single pass from the occlusal view. Considering the accuracy results, where the TS group also showed lower deviations, a more straightforward scanning process should also lead to better accuracy.

Limitations of the study included that the IOS model and software program have been identified as an influencing factor on scan accuracy,[63,64] so the use of other IOS models may lead to different results. Other limitations were the inclusion of only maxillary scans, the location and angulation of the implants, the selected environmental conditions (ambient lighting conditions and temperature), and the operator's skill and experience. Future research should focus on clinical studies with different IOS models, including mandibular scans and operators with high levels of expertise. Additionally, the evaluation of the misfit at the abutment-prosthesis level must be considered for future research to evaluate implant digital scan accuracy.

CONCLUSIONS

Based on the findings of the present clinical study, the following conclusions were drawn:

1. The scannable healing abutments tested obtained better accuracy of complete arch implant scans recorded by using the IOS tested when compared with the standard ISBs assessed.
2. The scannable healing abutments tested obtained lower scanning time and number of photograms of the complete arch implant scans recorded by using the IOS tested when compared with the standard ISBs assessed.

REFERENCES

1. Blatz MB, Conejo J. The current state of chairside digital dentistry and materials. *Dent Clin North Am*. 2019;63:175–197.
2. Michelinakis G, Apostolakis D, Kamposiora P, et al. The direct digital workflow in fixed implant prosthodontics: A narrative review. *BMC Oral Health*. 2021;21:37.
3. Kihara H, Hatakeyama W, Komine F, et al. Accuracy and practicality of intraoral scanner in dentistry: A literature review. *J Prosthodont Res*. 2020;64:109–113.
4. Suese K. Progress in digital dentistry: The practical use of intraoral scanners. *Dent Mater J*. 2020;39:52–56.
5. Siqueira R, Galli M, Chen Z, et al. Intraoral scanning reduces procedure time and improves patient comfort in fixed prosthodontics and implant dentistry: A systematic review. *Clin Oral Investig*. 2021;25:6517–6531.
6. Revilla-León M, Lanis A, Yilmaz B, et al. Intraoral digital implant scans: Parameters to improve accuracy. *J Prosthodont*. 2023;32:150–164.
7. Revilla-León M, Kois DE, Kois JC. A guide for maximizing the accuracy of intraoral digital scans. Part 1: Operator factors. *J Esthet Restor Dent*. 2023;35:230–240.
8. Revilla-León M, Kois DE, Kois JC. A guide for maximizing the accuracy of intraoral digital scans: Part 2-Patient factors. *J Esthet Restor Dent*. 2023;35:241–249.
9. Canullo L, Colombo M, Menini M, et al. Trueness of intraoral scanners considering operator experience and three different implant scenarios: A preliminary report. *Int J Prosthodont*. 2021;34:250–253.
10. Revell G, Simon B, Mennito A, et al. Evaluation of complete-arch implant scanning with 5 different intraoral scanners in terms of trueness and operator experience. *J Prosthet Dent*. 2022;128:632–638.
11. Pesce P, Bagnasco F, Pancini N, et al. Trueness of intraoral scanners in implant-supported rehabilitations: An in vitro analysis on the effect of operators' experience and implant number. *J Clin Med*. 2021;10:5917.
12. Revilla-León M, Jiang P, Sadeghpour M, et al. Intraoral digital scans-Part 1: Influence of ambient scanning light conditions on the accuracy (trueness and precision) of different intraoral scanners. *J Prosthet Dent*. 2020;124:372–378.
13. Ochoa-López G, Cascos R, Antonaya-Martín JL, et al. Influence of ambient light conditions on the accuracy and scanning time of seven intraoral scanners in complete-arch implant scans. *J Dent*. 2022;121:104138.
14. Ochoa-López G, Revilla-León M, Gómez-Polo M. Impact of color temperature and illuminance of ambient light conditions on the accuracy of complete-arch digital implant scans. *Clin Oral Implants Res*. 2024;35:898–905.
15. Mangano FG, Hauschild U, Veronesi G, et al. Trueness and precision of 5 intraoral scanners in the impressions of single and multiple implants: A comparative in vitro study. *BMC Oral Health*. 2019;19:101.
16. Gómez-Polo M, Cascos R, Ortega R, et al. Influence of arch location and scanning pattern on the scanning accuracy, scanning time, and number of photograms of complete-arch intraoral digital implant scans. *Clin Oral Implants Res*. 2023;34:591–601.
17. Li Z, Huang R, Wu X, et al. Effect of scan pattern on the accuracy of complete-arch digital implant impressions with two intraoral scanners. *Int J Oral Maxillofac Implants*. 2022;37:731–739.
18. Gómez-Polo M, Cascos R, Ortega R, et al. Influence of scanning pattern on accuracy, time, and number of photograms of complete-arch implant scans: A clinical study. *J Dent*. 2024;150:105310.
19. Gómez-Polo M, Donmez MB, Çakmak G, et al. Influence of implant scan body design (height, diameter, geometry, material, and retention system) on intraoral scanning accuracy: A systematic review. *J Prosthodont*. 2023;32:165–180.
20. Meneghetti PC, Li J, Borella PS, et al. Influence of scanbody design and intraoral scanner on the trueness of complete arch implant digital impressions: An in vitro study. *PLoS One*. 2023;18:e0295790.
21. Lawand G, Ismail Y, Revilla-León M, Tohme H. Effect of implant scan body geometric modifications on the trueness and scanning time of complete arch intraoral implant digital scans: An in vitro study. *J Prosthet Dent*. 2024;131:1189–1197.
22. Revilla-León M, Gómez-Polo M, Rutkunas V, et al. Classification of complete-arch implant scanning techniques recorded by using intraoral scanners. *J Esthet Restor Dent*. 2025;37:236–243.
23. Orejas-Perez J, Gimenez-Gonzalez B, Ortiz-Collado I, et al. In vivo complete-arch implant digital impressions: Comparison of the precision of three optical impression systems. *Int J Environ Res Public Health*. 2022;19:4300.
24. Koshiishi Y, Tanaka S, Iwauchi Y, Baba K. Impact of scanning range and image count on the precision of digitally recorded intermaxillary relationships in interocclusal record using intraoral scanner. *J Oral Sci*. 2024;66:111–115.
25. Morsy N, El Kateb M. In vivo precision of digital static interocclusal registration for full arch and quadrant arch scans: A randomized controlled clinical trial. *BMC Oral Health*. 2022;22:559.
26. Giannetti L, Apponi R, Mordini L, et al. The occlusal precision of milled versus printed provisional crowns. *J Dent*. 2022;117:103924.
27. Elkersh NM, Fahmy RA, Zayet MK, et al. The precision of two alternative indirect workflows for digital model production: An illusion or a possibility? *Clin Oral Investig*. 2023;27:3787–3797.
28. Menini M, Setti P, Pera F, et al. Accuracy of multi-unit implant impression: Traditional techniques versus a digital procedure. *Clin Oral Investig*. 2018;22:1253–1262.
29. Liu M, Fu XJ, Lai HC, et al. Accuracy of traditional open-tray impression, stereophotogrammetry, and intraoral scanning with prefabricated aids for implant-supported complete arch prostheses with different implant distributions: An in vitro study. *J Prosthet Dent*. 2024;132:602.e1–602.e9.
30. Ashry A, Abdelhamid AM, Ezzelarab S, Khamis MM. Effect of using scan body accessories and inter-implant distances on the accuracy of complete arch implant digital impressions: An in vitro study. *J Prosthodont* 2024.
31. Demirel M, Donmez MB, Şahmalı SM. Trueness and precision of mandibular complete-arch implant scans when different data acquisition methods are used. *J Dent*. 2023;138:104700.
32. Ali K, Alzaid AA, Suprono MS, et al. Evaluating the effects of splinting implant scan bodies intraorally on the trueness of complete arch digital scans: A clinical study. *J Prosthet Dent*. 2024;132:781.
33. Fu XJ, Liu M, Shi JY, et al. Comparison of different intraoral scanners with prefabricated aid on accuracy and framework passive fit of digital complete-arch implant impression: An in vitro study. *Clin Oral Implants Res*. 2025;26:17–27.
34. Vitai V, Németh A, Sólyom E, et al. Evaluation of the accuracy of intraoral scanners for complete-arch scanning: A systematic review and network meta-analysis. *J Dent*. 2023;137:104636.
35. Jeong M, Ishikawa-Nagai S, Lee JD, Lee SJ. Accuracy of impression scan bodies for complete arch fixed implant-supported restorations. *J Prosthet Dent* 2023.
36. Eid HS, Zohdy MM, Nour M, Salah T. A comparative analysis of the passivity of fit of complete arch implant-supported frameworks fabricated using different acquisition techniques. *J Prosthet Dent*. 2024;131:477.
37. Jemt T, Book K. Prosthesis misfit and marginal bone loss in edentulous implant patients. *Int J Oral Maxillofac Implants*. 1996;11:620–625.
38. Katsoulis J, Takeichi T, Sol Gaviria A, et al. Misfit of implant prostheses and its impact on clinical outcomes. Definition, assessment and a systematic review of the literature. *Eur J Oral Implantol*. 2017;10(1):121–138.
39. Paratelli A, Vania S, Gómez-Polo C, et al. Techniques to improve the accuracy of complete arch implant intraoral digital scans: A systematic review. *J Prosthet Dent*. 2023;129:844–854.
40. Pan Y, Dai X, Wan F, et al. A novel post-processing strategy to improve the accuracy of complete-arch intraoral scanning for implants: An in vitro study. *J Dent*. 2023;139:104761.
41. Revilla-León M, Smith Z, Methani MM, et al. Influence of scan body design on accuracy of the implant position as transferred to a virtual definitive implant cast. *J Prosthet Dent*. 2021;125:918–923.
42. Pachiou A, Zervou E, Tsirogiannis P, et al. Characteristics of intraoral scan bodies and their influence on impression accuracy: A systematic review. *J Esthet Restor Dent*. 2023;35:1205–1217.
43. Gehrke P, Rashidpour M, Sader R, Weigl P. A systematic review of factors impacting intraoral scanning accuracy in implant dentistry with emphasis on scan bodies. *Int J Implant Dent*. 2024;10:20.
44. Motel C, Kirchner E, Adler W, et al. Impact of different scan bodies and scan strategies on the accuracy of digital implant impressions assessed with an intraoral scanner: An in vitro study. *J Prosthodont*. 2020;29:309–314.
45. Etxaniz O, Amezua X, Jauregi M, Solaberrieta E. Improving the accuracy of complete arch implant intraoral digital scans by using horizontal scan bodies with occlusal geometry: A dental technique. *J Prosthet Dent*. 2025;133:57–61.
46. Atalay S, Çakmak G, Donmez MB, et al. Effect of implant location and operator on the accuracy of implant scans using a combined healing abutment-scan body system. *J Dent*. 2021;115:103855.
47. Abduo J, Lee CL, Sarfarazi G, et al. Encode protocol versus conventional protocol for single-implant restoration: A prospective 2-year follow-up randomized controlled trial. *J Oral Implantol*. 2021;47:36–43.
48. Abduo J, Chen C, Le Breton E, et al. The effect of coded healing abutments on treatment duration and clinical outcome: A randomized controlled

clinical trial comparing encode and conventional impression protocols. *Int J Oral Maxillofac Implants*. 2017;32:1172–1179.
49. Nayyar N, Yilmaz B, Mc Glumphy E. Using digitally coded healing abutments and an intraoral scanner to fabricate implant-supported, cement-retained restorations. *J Prosthet Dent*. 2013;109:210–215.
50. Agustín-Panadero R, Estada MIC, Alonso Pérez-Barquero J, et al. Effect of relative humidity on the accuracy, scanning time, and number of photograms of dentate complete arch intraoral digital scans. *J Prosthet Dent* 2025:865–871.
51. Limones A, Çakmak G, Fonseca M, et al. Impact of scanning interruptions on accuracy of implant-supported full-arch scans: An in-vitro pilot study. *J Dent*. 2025;153:105503.
52. Gómez-Polo M, Cimolai A, Ortega R, et al. Accuracy, scanning time, and number of photograms of various scanning patterns for the extraoral digitalization of complete dentures by using an intraoral scanner. *J Prosthet Dent*. 2024;131:521–528.
53. Ma J, Rubenstein JE. Complete arch implant impression technique. *J Prosthet Dent*. 2012;107:405–410.
54. Mangano FG, Admakin O, Bonacina M, et al. Trueness of 12 intraoral scanners in the full-arch implant impression: A comparative in vitro study. *BMC Oral Health*. 2020;20:263.
55. Hamilton A, Negreiros WM, Jain S, et al. Influence of scanning protocol on the accuracy of complete-arch digital implant scans: An in vitro study. *Clin Oral Implants Res*. 2024;35:641–651.
56. Vag J, Stevens CD, Badahman MH, et al. Trueness and precision of complete arch dentate digital models produced by intraoral and desktop scanners: An ex-vivo study. *J Dent*. 2023;139:104764.
57. Pozzi A, Agliardi E, Lio F, et al. Accuracy of intraoral optical scan versus stereophotogrammetry for complete-arch digital implant impression: An in vitro study. *J Prosthodont Res*. 2024;68:172–180.
58. Hamilton A, Negreiros WM, Jain S, et al. Influence of scanning protocol on the accuracy of complete-arch digital implant scans: An in vitro study. *Clin Oral Implants Res*. 2024;35:641–651.
59. Rutkūnas V, Gedrimienė A, Mischitz I, et al. EPA Consensus project paper: Accuracy of photogrammetry devices, intraoral scanners, and conventional techniques for the full-arch implant impressions: a systematic review. *Eur J Prosthodont Restor Dent* 2023.
60. Floriani F, Lopes GC, Cabrera A, et al. linear accuracy of intraoral scanners for full-arch impressions of implant-supported prostheses: A systematic review and meta-analysis. *Eur J Dent*. 2023;17:964–973.
61. Gómez-Polo M, Sallorenzo A, Cascos R, et al. Conventional and digital complete arch implant impression techniques: An in vitro study comparing accuracy. *J Prosthet Dent*. 2024;132:809–818.
62. Farah RI, Alresheedi B, Alazmi S, Al-Haj Ali SN. Evaluating the impact of scan body angulation and geometric attachments on the accuracy of complete-arch digital implant impressions: A comparison of two intraoral scanners. *J Prosthodont*. 2025;34:174–181.
63. Amornvit P, Rokaya D, Sanohkan S. Comparison of accuracy of current ten intraoral scanners. *Biomed Res Int*. 2021;2021:2673040.
64. Ender A, Zimmermann M, Mehl A. Accuracy of complete- and partial-arch impressions of actual intraoral scanning systems in vitro. *Int J Comput Dent*. 2019;22:11–19.

Corresponding author:
Dr Miguel Gómez-Polo
Department of Conservative Dentistry and Prosthodontics
School of Dentistry
Plaza Ramón y Cajal s/n
School of Dentistry
Complutense University of Madrid (UCM)
Madrid 28033
SPAIN
Email: mgomezpo@ucm.es

https://doi.org/10.1016/j.prosdent.2025.03.035